that except for 2,4,5-trithia[1.1.1]propellane, single determinant wave function treatments may not be appropriate for these species.

B. Germanium and Tin Compounds. Since ECP calculations compare favorably with full ab initio results, only ECP results are reported for the heavier atoms. The most interesting electronic structural features found for C and Si are those in the trioxa species, so we limit ourselves to these and omit discussion of the sulfur analogues. The results of structures, energetics, and the TCSCF NOON of the germanium and tin trioxa[1.1.1]propellane derivatives are listed in Tables I-IV along with the carbon and silicon analogues. Because the essential conclusions drawn for Ge and Sn compounds (**3** and **4** with M = Ge, Sn and L = O) are the same as those discussed above for C and Si, only the key features of these species will be addressed.

In both the germanium and tin analogues of **3** (L = O) extremely short bridgehead M-M distances are found at the RHF, ROHF, and TCSCF levels of theory. These bridgehead M-M distances are not significantly affected by the additions of hydrogens across the bridgehead centers (cf. Tables I and II). Indeed, the differences between the M-M distances in the propellanes **3** and the bicyclopentane **4** analogues are less than 0.1 Å for both M = Ge and Sn. Furthermore, differences among the three levels of theory (RHF, ROHF, and TCSCF) in the corresponding M-M bridgehead distances are within 0.1 Å. These results are similar to those found in the silicon analogues of **3** and **4**. The RHF/SBK(d) geometric results for **3** (M = Ge, L = O) and the corresponding bicyclopentane analogue are essentially identical with those calculated by Nagase and Kudo[13a] using the 3-21G(d) basis set at the RHF level of theory. The percent diradical character and the singlet-triplet splittings for Sn (28%, 22.0 kcal mol^{-1}) and Ge (25%, 29 kcal mol^{-1}) are also similar to those discussed above (36%, 20.7 kcal mol^{-1}) for the Si analogue of **3**.

IV. Conclusions

In this study, ab initio molecular orbital theory has been used to investigate the structure and bonding of sulfur and oxygen propellane derivatives (**3**) and their bicyclopentane analogues (**4**) with RHF, ROHF, and TCSCF wave functions. We have found that the M = Si, Ge, and Sn species possess unusually short bridgehead distances. However, this does not result in significant bonding interactions, as shown by the TCSCF calculations and total density plots. For M = C, TCSCF calculations and total density analyses suggest substantial bridgehead bonding only in the L = S system. We have found excellent agreement in structures and energetics between ECP calculations and the 6-31G(d) all-electron calculations.

Acknowledgment. The computations described in this work were performed on the North Dakota State University IBM 3090/200E vector computer, obtained in part with the aid of a joint study agreement between IBM and NDSU, and on the Cray-2 at the National Center for Supercomputing Applications, Champaign, Illinois. This work was supported in part by a grant from the National Science Foundation (CHE-8911911). We thank Walter Stevens, Morris Krauss, Harold Basch, and Paul Jasien for making their ECPs available to us prior to publication.

Rotational Energy Surfaces of Aza- and Phospha-1,3-butadienes. A Theoretical Study

Steven M. Bachrach* and Meixiao Liu

Contribution from the Department of Chemistry, Northern Illinois University, DeKalb, Illinois 60115. *Received April 15, 1991*

Abstract: The rotational energy surfaces of all stereoisomers of 1-aza-, 2-aza-, 1,3-diaza-, 1,4-diaza-, and 2,3-diaza-1,3-butadienes and 1-phospha-, 2-phospha-, 1,3-diphospha-, 1,4-diphospha-, and 2,3-diphospha-1,3-butadienes were calculated at the MP2/6-31G*//HF/6-31G* level. Rotational barriers and all local minima were rigorously located and identified. For all systems except *anti*-1,3-diaza-1,3-butadiene, the *trans* conformer is the global minimum. Stable *gauche* isomers are present for most azabutadienes and all phosphabutadienes. Rotational barriers for the azabutadienes are between 1.4 and 8.6 kcal mol^{-1} and between 3.1 and 8.1 kcal mol^{-1} for the phosphabutadienes. The shapes and relative heights of the critical points on the rotational surfaces are discussed in terms of π-delocalization, 1,4-steric interactions, and intramolecular hydrogen bonding. The low rotational barriers and stable *gauge* conformers of the phosphabutadienes indicate that these molecules should undergo electrocyclic and cycloaddition reactions that require *cis*-like conformations of the diene.

Although the degree of delocalization of π-electrons through conjugation is a matter of some controversy,[1] the conformational preference for extended planar systems does support its existence. Both experimental[2-8] and theoretical[9-15] studies conclude that the lowest energy conformation is planar with an *s-trans* arrangement about the C-C single bond. The nature of the second stable conformer, about 2.5-4.0 kcal mol^{-1} higher in energy, is disputed. IR[5] and Raman[2] spectroscopy suggest a cis planar minimum,

(1) Popov, E. M.; Kogan, G. A. *Russ. Chem. Rev.* **1968**, *37*, 119-141.
(2) Carreira, L. A. *J. Chem. Phys.* **1975**, *62*, 3851-3854.
(3) Durig, J. R.; Bucy, W. E.; Cole, A. R. H. *Can. J. Phys.* **1975**, *53*, 1832-1837.
(4) Squillacote, M. E.; Sheridan, R. S.; Chapman, O. L.; Anet, F. A. L. *J. Am. Chem. Soc.* **1979**, *101*, 3657-3659.
(5) Furukawa, Y.; Takeuchi, H.; Harada, I.; Tasumi, M. *Bull. Chem. Soc. Jpn.* **1983**, *56*, 392-399.
(6) Squillacote, M. E.; Semple, T. C.; Mui, P. W. *J. Am. Chem. Soc.* **1985**, *107*, 6842-6846.
(7) Fischer, J. J.; Michl, J. *J. Am. Chem. Soc.* **1987**, *109*, 1056-1059.
(8) Arnold, B. R.; Balaji, V.; Michl, J. *J. Am. Chem. Soc.* **1990**, *112*, 1808-1812.
(9) Breulet, J.; Lee, T. J.; Schaefer, H. F., III *J. Am. Chem. Soc.* **1984**, *106*, 6250-6253.
(10) Bock, C. W.; George, P.; Trachtman, M. *Theor. Chim. Acta* **1984**, *64*, 293-311.
(11) De Mare, G. R.; Neisius, D. *J. Mol. Struct. (THEOCHEM)* **1984**, *109*, 103-126.
(12) Rice, J. E.; Liu, B.; Lee, T. J.; Rohlfing, C. M. *Chem. Phys. Lett.* **1989**, *161*, 277-284.
(13) Bock, C. W.; Panchenko, Y. N. *J. Mol. Struct. (THEOCHEM)* **1989**, *187*, 69-82.
(14) Wiberg, K. B.; Rosenberg, R. E. *J. Am. Chem. Soc.* **1990**, *112*, 1509-1519.
(15) Guo, H.; Karplus, M. *J. Chem. Phys.* **1991**, *94*, 3679-3699.

0002-7863/91/1513-7929$02.50/0

though a shallow well is likely.[3] UV spectroscopy of 1,3-butadiene in an Ar matrix suggests the dihedral angle must be less than 15°.[4,6] More recent polarized IR spectroscopy agrees with the UV prediction of a very small dihedral angle.[7,8] On the other hand, most[16] theoretical calculations[9-15] have indicated a stable *gauche* structure with dihedral angle φ = 36–40°, though the properties of the *gauche* and *cis* conformers may be quite similar.[12] The planar cis conformer is a transition state (one imaginary frequency).[9,12,14] Arnold, Balaji, and Michl[8] have suggested a simple reconciliation (but with reservations): different phases are being compared. Theory assumes an isolated single molecule while the experiments are performed on molecules in the condensed phase. The nature of the second conformer remains an active area of debate.

Conjugated phosphaalkenes have been known for the past decade. Examples of all positional isomers of mono-,[17,18] di-,[19-24] and triphospha-1,3-butadienes[25,26] have been prepared. Following the examples of the previously synthesized phosphaalkenes, these conjugated systems have bulky substituents to prevent dimerization.[27-29] Nevertheless, 1-phospha-1,3-butadienes will undergo [2 + 2] and [4 + 2] dimerizations unless a very large substituent (2,4,6-tri-*tert*-butylphenyl) is attached to the P.[17] 1,4-Diphospha-1,3-butadiene will undergo an intramolecular [2 + 2] cyclization[19] unless large substituents are present.[23] Somewhat surprisingly, no Diels–Alder reaction with the phospha-1,3-butadienes acting as the diene fragment has been discovered. A substituted 2-phospha-1,3-butadiene will act as the dienophile with cyclopentadiene.[17] This lack of cycloaddition chemistry has been explained in terms of the phospha-1,3-butadienes possessing a locked *s-trans* conformation and the *s-cis* is needed for cycloadditions to occur.[20,23] Our concern here is if the phospha-1,3-butadienes are inherently locked into the *s-trans* conformation or if the large substituents are forcing this arrangement.

We have been interested in the theoretical description of organophosphorus compounds, particularly the phosphaalkenes.[30-33] This paper presents the ab initio rotational energy surfaces of all isomers of mono- and diphospha-1,3-butadienes. The structures of all critical points on these surfaces are examined and energy barriers obtained to address the question of possible conformational rigidity. The effect of these surfaces in terms of pericyclic reactions is addressed. We also compare these surfaces with the parent compound (1,3-butadiene) and the nitrogen analogue and explain the striking differences in surface topology based on the very different structural features, electronegativity, and π-delocalization ability of P, N, and C. Since little work on the parent aza-1,3-butadienes[34-40] has been reported and no unsubstituted phospha-1,3-butadiene has been discussed in the literature, the rotational surfaces also provide the relative energies and structures of possible isomers that may be detected in the future.

Table I. Relative Energies (kcal mol^{-1}) Using HF/6-31G* Optimized Geometries

N compd	*E*(HF)	*E*(MP2)	P compd	*E*(HF)	*E*(MP2)
1NTA	0.0	0.0	**1PTS**	0.0	0.0
1NCA	2.82	2.55	**1PGS**	3.48	2.87
1NTS	0.87	0.82	**1PTA**	0.26	0.19
1NGS	3.63	3.18	**1PGA**	3.50	2.82
2NT	0.0	0.0	**2PT**	0.0	0.0
2NG	2.07	1.23	**2PG**	2.76	2.08
13NTS	0.0	0.0	**13PTS**	0.0	0.0
13NGS	2.28	1.33	**13PGS**	2.60	1.73
13NTA	3.09	2.81	**13PTA**	1.05	1.22
13NGA	1.03	0.58	**13PGA**	2.90	2.17
14NTAA	0.0	0.0	**14PTAA**	0.0	0.0
14NGAA	8.09	7.46	**14PGAA**	4.31	3.11
14NTAS	2.38	1.99	**14PTSS**	0.08	0.01
14NCAS	3.12	2.01	**14PGSS**	4.33	3.23
14NTSS	3.46	2.78	**14PTAS**	0.08	0.07
14NGSS	6.06	4.78	**14PGAS**	4.20	3.04
23NT	0.0	0.0	**23PT**	0.0	0.0
23NC	16.66	15.02	**23PG**	3.80	3.05

Table II. Energies (kcal mol^{-1}) Relative to the T Conformer at MP2/6-31G*//HF/6-31G*

	T to G Barrier	T to G	T to C
	N Compounds		
1NS	5.62	2.36	2.74
1NA	7.38[a]		2.55
2N	3.73	1.23	5.37
13NS	2.18	1.33	5.68
13NA	1.38	−2.23	−1.6
14NSS	5.22	2.0	2.28
14NAA	8.64	7.46	7.58
14NAS	6.25[a]		0.02
23N			15.02
	P Compounds		
1PS	7.08	2.87	3.44
1PA	6.84	2.63	3.57
2P	3.59	2.06	4.88
13PS	3.14	1.78	3.32
13PA	3.29	0.96	2.7
14PSS	6.9	3.22	3.96
14PAA	8.08	3.11	4.67
14PAS	7.39	2.97	3.77
23P	3.45	3.05	6.17

[a] T to C barrier.

Computational Methods

All calculations were performed with either GAUSSIAN-85,[41] GAUSSIAN-86,[42] or GAUSSIAN-90[43] with the 6-31G* basis set. All geometric

(16) For a contrary conclusion, see: Feller, D.; Davidson, E. R. *Theor. Chim. Acta* **1985**, *68*, 57–67.
(17) Appel, R.; Knoch, F.; Kunze, H. *Chem. Ber.* **1984**, *117*, 3151–3159.
(18) Boyd, B. A.; Thoma, R. J.; Neilson, R. H. *Tetrahedron Lett.* **1987**, *28*, 6121–6124.
(19) Appel, R.; Barth, V. *Tetrahedron Lett.* **1980**, *21*, 1923–1924.
(20) Appel, R.; Barth, V.; Knoch, F. *Chem. Ber.* **1983**, *116*, 938–950.
(21) Markl, G.; Sejpka, H. *Tetrahedron Lett.* **1986**, *27*, 171–174.
(22) Appel, R.; Folling, P.; Schuhn, W.; Knoch, F. *Tetrahedron Lett.* **1986**, *27*, 1661–1664.
(23) Appel, R.; Hunerbein, J.; Siabalis, N. *Angew. Chem., Int. Ed. Engl.* **1987**, *26*, 779–780.
(24) Niecke, E.; Metternich, H. J.; Streubel, R. *Chem. Ber.* **1990**, *123*, 67–69.
(25) Appel, R.; Niemann, B.; Schuhn, W.; Knoch, F. *Angew. Chem., Int. Ed. Engl.* **1986**, *25*, 932.
(26) Appel, R.; Niemann, B.; Nieger, M. *Angew. Chem., Int. Ed. Engl.* **1988**, *27*, 957–958.
(27) Appel, R.; Knoll, F.; Ruppert, I. *Angew. Chem., Int. Ed. Engl.* **1981**, *20*, 731–744.
(28) Appel, R. *Pure Appl. Chem.* **1987**, *59*, 977–982.
(29) Markovski, L. N.; Romanenko, V. D. *Tetrahedron* **1989**, *45*, 6019–6090.
(30) Bachrach, S. M. *J. Comput. Chem.* **1989**, *10*, 392–406.
(31) Bachrach, S. M.; Liu, M. *Phosphorus Sulfur* **1990**, *53*, 7–13.
(32) Bachrach, S. M. *J. Org. Chem.* **1991**, *56*, 2205–2209.
(33) Bachrach, S. M.; Liu, M. *J. Phys. Org. Chem.* **1991**, *4*, 242–250.
(34) Penn, R. E. *J. Mol. Spectrosc.* **1978**, *69*, 373–382.
(35) Hamada, Y.; Tsuboi, M.; Matsuzawa, T.; Yamanouchi, K.; Kuchitsu, K.; Koga, Y.; Kondo, S. *J. Mol. Spectrosc.* **1984**, *105*, 453–464.
(36) Panchenko, Y. N.; Krasnoshchiokov, S. V.; Bock, C. W. *J. Comput. Chem.* **1988**, *9*, 443–454.
(37) Amatatsu, Y.; Hamada, Y.; Tsuboi, M. *J. Mol. Spectrosc.* **1987**, *123*, 276–285.
(38) Bock, C. W.; George, P.; Trachtman, M. *J. Comput. Chem.* **1984**, *5*, 395–410.
(39) Bondybey, V. E.; Nibler, J. W. *Spectrochim. Acta* **1973**, *29A*, 645–658.
(40) Hagen, K.; Bondybey, V.; Hedberg, K. *J. Am. Chem. Soc.* **1977**, *99*, 1365–1368.
(41) Hout, R. F., Jr.; Francl, M. M.; Kahn, S. D.; Dobbs, K. D.; Blurock, E. S.; Pietro, W. J.; McGrath, M. P.; Steckler, R.; Hehre, J. University of Illinois (Urbana—Champaign) and University of California (Irvine), 1988.
(42) Frisch, M.; Binkley, J. S.; Schlegel, H. B.; Raghavachari, K.; Martin, R.; Stewart, J. J. P.; Bobrowitz, F.; DeFrees, D.; Seeger, R.; Whiteside, R.; Fox, D.; Fluder, E.; Pople, J. A. Carnegie-Mellon University, 1986.

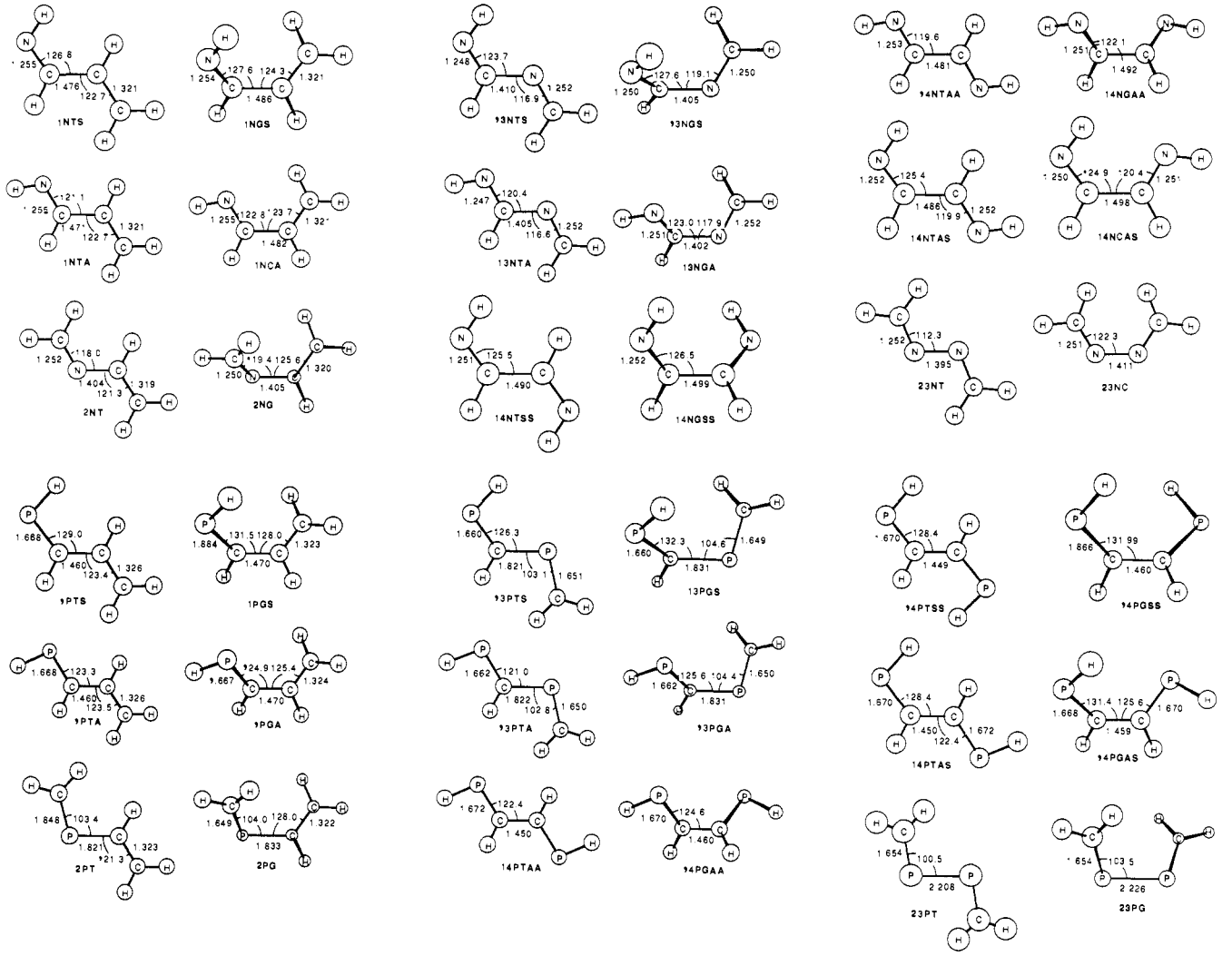

Figure 1. Optimized HF/6-31G* structures. All distances are in Å and all angles are in deg.

isomers of all mono- and di-substituted aza- and phosphabutadienes were examined. The nitrogen-substituted molecules are 1-aza-1,3-butadiene with the N-H bond anti (**1NA**) or syn (**1NS**) to the C=N bond, 2-aza-1,3-butadiene (**2N**), 1,3-diaza-1,3-butadiene with the N-H bond anti (**13NA**) or syn (**13NS**) to the C=N bond, 1,4-diaza-1,3-butadiene with the two N-H bonds anti (**14NAA**) or syn (**14NSS**) or one bond syn and the other anti (**14NAS**). and 2,3-diaza-1,3-butadiene (**23N**). The phosphorus analogues are designated similarly with **P** replacing **N**.

The 6-31G* basis set is only moderate in size; however, our previous calculations of organophosphorus systems indicate that it satisfactorily reproduces the geometries of phosphaalkenes.[30] Comparisons between calculated and experimental structures of the aza- and phosphabutadienes are limited by the small number of experimental studies, particularly of the parent compounds. Nevertheless, the agreement between the limited experimental results and our calculations is quite good (see below). While larger basis sets will undoubtedly alter the geometries, we believe that expansion of the basis set will result in only small changes that should not seriously affect our analysis.

The rotational surfaces were generated by complete geometry optimization with the dihedral angle (φ) about the single bond between atoms 2 and 3 fixed at 30.0° increments with φ = 0.0° and 180.0° corresponding to the *s-cis* (C) and *s-trans* (T) conformers, respectively. For some compounds, other intermediate dihedral angles were also examined to refine the rotational structure. For many structures, the C conformer is a transition state, confirmed by the presence of one and only one negative eigenvalue of the Hessian matrix, connecting mirror image

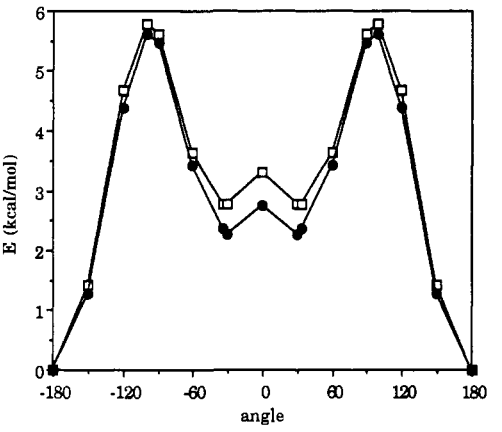

Figure 2. Rotational energy surface of **1NS**: (□) HF/6-31G*, (●) MP2.

gauche structures. These *gauche* (G) structures were fully optimized and found to be local minima by analytical frequency analysis. The rotational barriers between the T structure and either the G or C structure were also fully optimized. Drawings of all the local minima structures with pertinent geometric parameters are shown in Figure 1. Relative energies are listed in Table I. Since many of the rotational surfaces are structurally quite similar, only representative examples are included in this paper. These plots are shown in Figures 2-6.

The effects of electron correlation were examined by single-point energy calculations at the MP2 level using the HF structures. These calculations are designated MP2/6-31G*//HF/6-31G*. Relative energies are given in Tables I and II. In general, the rotational surface was relatively unaffected by the inclusion of correlation (see Figures 2-6),

(43) Frisch, M. J.; Head-Gordon, M.; Trucks, G. W.; Foresman, J. B.; Schlegel, H. B.; Raghavachari, K.; Robb, M. A.; Binkley, J. S.; Gonzalez, C.; DeFrees, D. J.; Fox, D. J.; Whiteside, R. A.; Seeger, R.; Melius, C. F.; Baker, J.; Martin, R. L.; Kahn, L. R.; Stewart, J. J. P.; Topiol, S.; Pople, J. A. Gaussian, Inc.: Pittsburgh, PA, 1990.

(44) Hamilton, W. C.; Ibers, J. C. *Hydrogen Bonding in Solids*; W. A. Benjamin: New York, 1968; p 16.

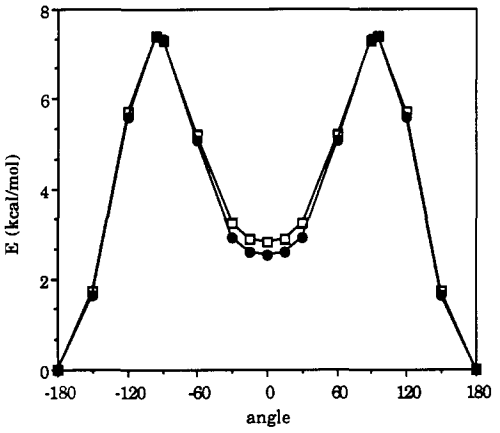

Figure 3. Rotational energy surface of 1NA: (□) HF/6-31G*, (●) MP2.

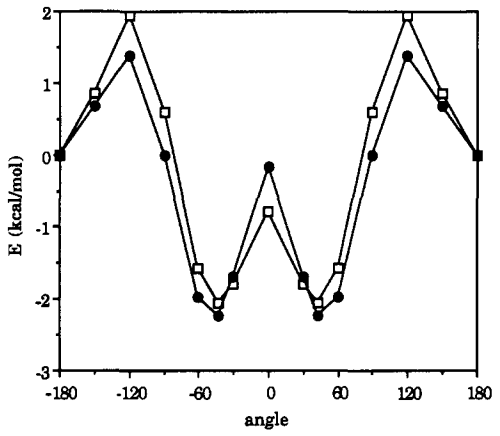

Figure 4. Rotational energy surface of 13NA: (□) HF/6-31G*, (●) MP2.

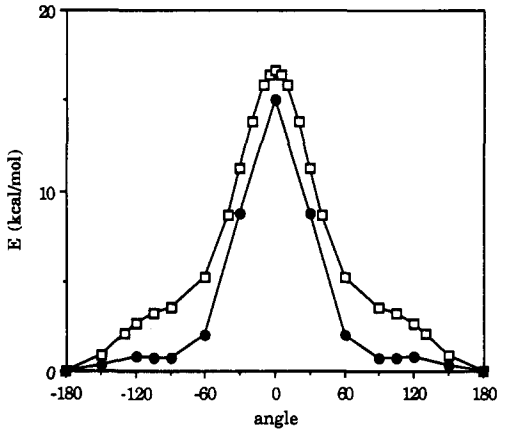

Figure 5. Rotational energy surface of 23N: (□) HF/6-31G*, (●) MP2.

as has been observed in previous studies of rotational surfaces of 1,3-butadienes.[10,13,14]

Results

Aza-1,3-butadienes. (a) 1-Aza-1,3-butadiene (1NA and 1NS). 1-Aza-1,3-butadiene has been characterized by Penn[34] using microwave spectroscopy and Hamada et al. using IR spectroscopy.[35] Penn assumed that the *s-trans* species would dominate and solved the **1NTA** structure, but lacked sufficient spectral lines to determine the **1NTS** structure. He estimated that **1NTA** is 0.88 kcal mol^{-1} more stable than **1NTS** and about 2.3 kcal mol^{-1} more stable than **1NCA**. The IR work supported Penn's conclusions, as did calculations[36] at the HF/6-31G* (5 d functions) level. This calculational work did not consider **1NCS**, since it should be remotely high in energy.

The optimized local minima structures are shown in Figure 1. The calculated geometry of **1NTA** agrees well with the experimental bond distances (C=C, 1.336 Å; C-C, 1.454 Å; C=N, 1.274 Å) and angles (C-C-C, 122.9°; N-C-C, 121.5°). The optimized structures of Bock are very similar to our results; the slight differences are due to our basis set having 6 d functions. The energy difference between **1NTA** and **1NTS** is 0.82 kcal mol^{-1}, with **1NCA** lying 2.55 kcal mol^{-1} above **1NTA**, both essentially identical with the experimental findings. **1NCS** is a transition state (TS) connecting the mirror image **1NGS** conformers. This conformer is 3.18 kcal mol^{-1} less stable than **1NTA** and is unlikely to exist in appreciable quantity in the gas phase.

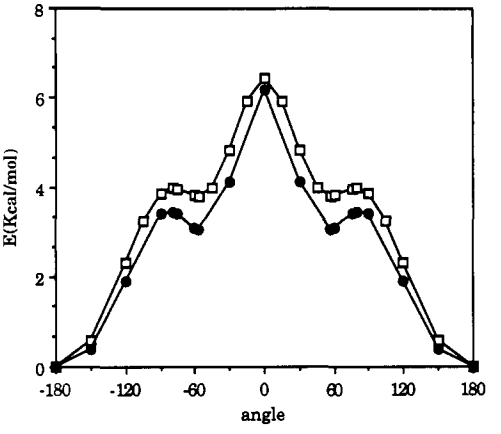

Figure 6. Rotational energy surface of 23P: (□) HF/6-31G*, (●) MP2.

The rotational surfaces of **1NS** and **1NA** are shown in Figures 2 and 3, respectively. The surface of **1NS** is quite typical of most 1,3-butadienes, including the parent hydrocarbon[10,13,14] itself. The surface has four critical points corresponding to two local minima and two transition states. The overall shape of the surface is not altered by incorporation of electron correlation. The *s-trans* conformer (φ = 180°) is the lowest energy form. A barrier to rotation (5.62 kcal mol^{-1}) about the C2-C3 bond appears at φ = 98.87°. A local minimum at φ = 34.43° lies 2.36 kcal mol^{-1} above the trans form. The mirror image of this gauche form is separated by another barrier which is the *s-cis* planar structure. This *cis* conformer is 2.74 kcal mol^{-1} above the trans form, making a barrier of 0.38 kcal mol^{-1} between the gauche forms. This general shape is also found for the parent hydrocarbon 1,3-butadiene, many of the azabutadienes, and all of the phosphabutadienes examined in this work. Only the relative energies of the critical points vary from one structure to another. These energies are given in Table II.

The rotational surface of **1NA** (Figure 3) differs from the standard surface in that there is no *gauche* structure and the *s-cis* conformer is a local minimum. The barrier separating the T and C conformers occurs at φ = 95.66° and is 7.38 kcal mol^{-1}. **1NCA** is 2.55 kcal mol^{-1} less stable than **1NTA**.

(b) 2-Aza-1,3-butadiene (2N). 2-Aza-1,3-butadiene has been detected by FTIR in the gas phase and many bands were assigned with the aid of HF/4-31G* optimized structures of the T and C conformers.[37] Bock, George, and Trachtman[38] characterized the rotational surface of **2N** at HF/6-31G* (5 d functions). Their surface clearly indicates a stable *gauche* structure, but this conformer was not located. They found **2NC** to lie 5.74 kcal mol^{-1} above **2NT** at HF/6-31G*, and the difference decreases about 1.5 kcal mol^{-1} at MP2. Their estimate of the barrier between **2NT** and **2NG** is 4.11 kcal mol^{-1}, which also decreases by about 1.5 kcal mol^{-1} with inclusion of correlation.

The HF/6-31G* optimized geometries of **2NT** and **2NG** are drawn in Figure 1. As expected, the **2NT** structure is nearly identical with Bock's structure. The dihedral angle in **2NG** is 54.75°. All other geometrical parameters of **2NT** and **2NG** are quite similar to each other except the C-C-N angle is larger in the more crowded *gauche* conformer.

The rotational surface of **2N** is isomorphic with the one shown in Figure 2. The global minimum is **2NT** and the other local minimum is **2NG**, which lies 1.23 kcal mol^{-1} higher in energy. The barrier separating these two minima occurs at φ = 98.87° and

lies 3.73 kcal mol^{-1} above **2NT**. **2NC** is the transition structure connecting the **2NG** conformers and forms a barrier of 4.14 kcal mol^{-1}.

(c) 1,3-Diaza-1,3-butadiene (13NA and 13NS). 1,3-Diaza-1,3-butadiene has not been observed and no theoretical studies have been reported. The optimized *trans* and *gauche* conformational geometries for both **13NA** and **13NS** are drawn in Figure 1. Bond distances and angles for these structures are typical. **13NTS** is the lowest energy isomer, but the other local minima lie close above (see Table I) and all may be accessible.

The rotational surface for **13NS** is isomorphic with the one shown in Figure 2. The *trans* conformer is the global minimum. The dihedral angle of the *gauche* form is 62.21° and the barrier between it and the *trans* conformer occurs at φ = 105.90°. **13NGS** lies 1.33 kcal mol^{-1} above **13NTS**, the rotational barrier is 2.18 kcal mol^{-1}, and **13NCS** (the barrier separating the mirror image *gauche* forms) is 4.35 kcal mol^{-1} above **13NGS**.

The rotational energy surface of **13NA** is shown in Figure 4. While the shape of this surface is similar to the one in Figure 2, the *trans* conformer is not the global minimum; rather, the *gauche* form (φ = 42.84°) is the local minimum, lying 2.23 kcal mol^{-1} below **13NTA**. **13NCA** is the transition state for rotational conversion of the two mirror *gauche* forms and is 2.07 kcal mol^{-1} above **13NGA**. The barrier separating **13NTA** and **13NGA** has φ = 120.00° and is 3.51 kcal mol^{-1} above **13NGA**.

(d) 1,4-Diaza-1,3-butadiene (14NAA, 14NSS, and 14NAS). No reports of 1,4-diaza-1,3-butadiene have been published. The relative energies of all stable isomers are listed in Table I. The most stable isomer is **14NTAA** with the *cis* and *trans* forms of **14NAS** lying about 2 kcal mol^{-1} higher.

The optimized geometries of all stable isomers of **14N** are shown in Figure 1. The geometric trends for these compounds are identical with those of all the other butadienes. The C2–C3 bond is shorter in the *trans* conformer than in the *gauche* or *cis* forms. The heavy-atom bond angles are larger in G and C than in T.

The rotational energy surfaces of **14NAA** and **14NSS** are isomorphic with the surface shown in Figure 2. For **14NSS**, the *trans* isomer is 2.00 kcal mol^{-1} more stable than the *gauche* isomer (φ = 31.27°). The rotational barrier between these two occurs at φ = 95.21° and is 5.22 kcal mol^{-1}. The *cis* structure lies 0.28 kcal mol^{-1} above the *gauche* conformer and is the transition state for interconversion of the mirror image *gauche* conformers. This barrier is quite small, and spectroscopic observation of a second rotamer of **14NSS** will likely indicate it to be *cis* planar.

14NGAA occurs with φ = 33.30° and is 7.46 kcal mol^{-1} less stable than **14NTAA**. The barrier (φ = 78.90°) to conversion of these two is 8.64 kcal mol^{-1} above **14NTAA**. Thus, it is unlikely that **14NGAA** will be observed. Interconversion of the *gauche* structures crosses a barrier (**14NCAA**) of only 0.12 kcal mol^{-1}.

The rotational surface of **14NAS** is similar to that shown in Figure 3. **14NTAS** and **14NCAS** are essentially degenerate. The barrier separating them occurs at φ = 94.93° and is 6.25 kcal mol^{-1}.

(e) 2,3-Diaza-1,3-butadiene (23N). 2,3-Diaza-1,3-butadiene has been examined in the gas phase with IR, Raman spectroscopy, and electron diffraction techniques.[39,40] These studies suggested a dominant *trans* conformation, with as much as 25% of a second isomer at 225 °C. By assuming a rigid-rotor-like structure where the molecule only changes the dihedral angle φ, a *gauche* conformation was suggested for the second isomer with $\varphi \approx 60°$. The electron diffraction structure indicated C=N and N—N bond lengths of 1.277 and 1.418 Å, respectively, and a C–N–N angle of 111.4°. The *trans* to *gauche* energy difference (obtained by using a three-term cosine expansion potential) is 1.2 kcal mol^{-1}, the barrier separating them is 1.5 kcal mol^{-1}, and the *cis* conformer is 0.53 kcal mol^{-1} above the *gauche* form.

Bock, George, and Trachtman examined the rotational surface of **23N** at the HF/6-31G* (5 d functions).[38] They could find no local minimum corresponding to a *gauche* rotamer, but they did notice that the surface was quite flat in the region φ = 80–110°. This plateau lies about 3.5 kcal mol^{-1} above **23NT**. The only minimum is **23NT**, and **23NC** is a transition state 16.53 kcal mol^{-1} higher in energy. The two proposals made by Bock et al. to account for the differences in the experimental and theoretical results were (a) the propensity for calculations to overestimate lone-pair–lone-pair repulsion and (b) the inadequacy of the 3-term potential function and the rigid-rotor model used in the experimental work. The former was somewhat discounted, due to the lack of change in the potential surface with inclusion of correlation at MP2 and MP3. The latter proposal does merit serious attention. Adequate accounting of the rotational surface of 1,3-butadiene requires at least a four-term, if not a six-term, potential. Bock, George, and Trachtman report the geometries of **23NT** and **23NC** and sizable differences are evident. The C–N–N angle in **23NC** is 11° larger and the N–N distance is 0.016 Å larger than in **23NT**.

The HF/6-31G* optimized structures of **23NT** and **23NC** differ only slightly from Bock's structures.[38] Thus, significant structural changes accompany rotation about the N–N bond (see below). The calculated structure of **23NT** agrees well with the electron diffraction structure, except for the N–N bond which is predicted to be 0.013 Å longer.

The rotational energy surface of **23N** is shown in Figure 5. At the HF-SCF level, the only critical points are **23NT**, which is the global minimum, and **23NC**, a transition state. A plateau region is found between 80° and 110°. However, at the MP2/6-31G*//HF/6-31G* level, an extremely shallow minimum between 90° and 105° is evident. This region is only 0.7 kcal mol^{-1} above **23NT** and is separated from **23NT** by a very small barrier. The transition state **23NC** lies 15.02 kcal mol^{-1} above **23NT**.

Phospha-1,3-butadienes. No unsubstituted phospha-1,3-butadienes have been prepared. Unsubstituted phosphaalkenes tend to dimerize rapidly, which is usually prevented by adding bulky substituents to both C and P. This same approach has been taken to synthesize and isolate a number of phospha-1,3-butadienes.

For reference comparison with the calculated structures reported below, typical P=C distances from X-ray crystal structure determination range from 1.68 to 1.72 Å and P—P distances range from 2.21 to 2.23 Å.[20] Typical ranges for P—C and P=C distances, calculated at HF/6-31G*, are 1.832–1.868 and 1.647–1.669 Å, respectively.[30]

(a) 1-Phospha-1,3-butadiene (1PA and 1PS). A number of substituted 1-phospha-1,3-butadienes have been prepared, but only two, **1a**[17] and **1b**,[18] have been isolated and characterized. Other 1-phospha-1,3-butadienes undergo self-Diels–Alder or [2 + 2] cycloaddition reactions under the same conditions in which they are formed, and their intermediacy is inferred by analogy with hydrocarbon chemistry.[17] No geometric data for either compound are available.

R~P=CHR′—CH=CHR″

	R	R′	R″
1a	2,3,5-tri(*tert*-butyl)phenyl	OTMS	phenyl
1b	$(TMS)_2N$	TMS	TMS

The geometries of the *trans* and *gauche* conformers **1PA** and **1PS** are drawn in Figure 1. The P=C distance is at the high end of the range for typical P=C bonds. The C—C distance is longer in the *gauche* forms than in the *trans* forms, which reflects perhaps less π-delocalization and/or relief of steric congestion. This latter effect certainly accounts for the wider backbone angles in the *gauche* rotamers.

The energies of **1PTS** and **1PTA** are nearly equal, with the former slightly more stable. The *gauche* conformers are about 2.8 kcal mol^{-1} less stable than their *trans* conformers.

The rotational surface for both **1PA** and **1PS** is isomorphic with the surface shown in Figure 2. (Recall that the surface for **1NA** differs in shape and is shown in Figure 3.) The rotational barrier separating **1PTS** from **1PGS** (φ = 34.31°) occurs at φ = 99.71° and is 7.08 kcal mol^{-1}, while the barrier separating **1PTA** from **1PGA** (φ = 37.38°) occurs at φ = 102.66° and is 6.84 kcal mol^{-1}. **1PCS** and **1PCA** are both transition states, lying 0.57 and 0.94 kcal mol^{-1}, respectively, above their *gauche* conformers.

(b) 2-Phospha-1,3-butadiene (2P). Appel and co-workers[17] have prepared and isolated two substituted 2-phospha-1,3-butadienes,

2a and **2b**, though no geometric data have been reported. Neither analogue underwent any Diels–Alder or [2 + 2] reaction as the diene fragment, though the P=C did act as the dienophile toward cyclopentadiene in a Diels–Alder reaction.

Ph—CH=CH—P=C(R)OTMS

2a: R = Ph
2b: R = *t*-Bu

The optimized structures of **2PT** and **2PG** are drawn in Figure 1. The P=C bond length lies within the range of calculated distances, while the P—C bond length of 1.821 Å in **2PT** is shorter than typical P—C distances. The P—C distance is longer in **2PG**, lying within the range for typical distances. The dihedral angle in **2PG** is 46.55°. As for all phosphabutadienes, the single bond connecting positions 2 and 3 is longer in the *gauche* conformer than in the trans form, reflecting deminished π-delocalization and/or increased steric crowding.

P2G lies 2.06 kcal mol^{-1} above **2PT** with a rotational barrier of 3.59 kcal mol^{-1} (at φ = 94.06°) between them. The one unusual feature of the rotational surface of **2P** is that **2PC**, which is the transition state connecting the mirror *gauche* conformers, is higher in energy than the rotational barrier between **2PT** and **2PG**. **2PC** lies 4.88 kcal mol^{-1} above **2PT** or, in other terms, 2.82 kcal mol^{-1} above **2PG**.

(c) 1,3-Diphospha-1,3-butadiene (13PA and 13PS). There are three reports of substituted 1,3-diphospha-1,3-butadienes. The first was **3a**, which was not isolated, but rather underwent an electrocyclic ring closure to give the 1,3-diphosphacyclobutene.[20] A few years later, Appel and co-workers[22] reported the synthesis and X-ray structure of **3b**. This structure indicated an *s-trans* conformation and an *anti* arrangement about the P=C bond. The P(1)=C(2), C(2)—P(3), and P(3)=C(4) distances are 1.696, 1.845, and 1.696 Å, respectively, and the P(1)–C(2)–P(3) and C(2)–P(3)–C(4) angles are 107.4° and 110.3°, respectively. The last reported analogue **3c** was again not isolated, but inferred as an intermediate in the synthesis of a diphosphabicyclobutane.[24]

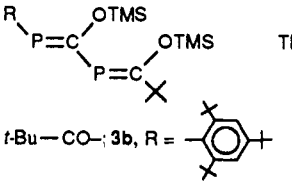

3a, R = *t*-Bu—CO–; **3b**, R =

TMS—P=C(TMS)—P=C(TMS)$_2$

3c

The HF/6-31G* optimized structures of **13PTS**, **13PGS**, **13PTA**, and **13PGA** are drawn in Figure 1. Comparison of the geometry of **13PTA** with the crystal structure of **3b** is difficult due to the difference in substitution and phase. The bond lengths in **3b** are all longer than in the calculated structure, but are in reasonable agreement. The bond angles are quite different, which likely is caused by the dramatically different steric requirements of **3b** and **13PTA**. **13PTS** is 1.22 kcal mol^{-1} more stable than **13PTA**. The preference for a *syn* arrangement about the P=C bond is well-established.

The rotational surfaces of **13PS** and **13PA** are standard. For the former, **13PGS** occurs at φ = 48.62° and is 1.78 kcal mol^{-1} above **13PTS**. The barrier separating these two conformers occurs at φ = 95.09 and is 3.14 kcal mol^{-1}. The *cis* conformer is 1.54 kcal mol^{-1} above **13PGS**. **13PGA** lies 0.96 kcal mol^{-1} above **13PTA** and its dihedral angle is 45.98°. The rotational maximum occurs at φ = 101.04° and imposes a barrier of 3.29 kcal mol^{-1}. The *cis* conformer is 1.74 kcal mol^{-1} above the *gauche* form.

(d) 1,4-Diphospha-1,3-butadiene (14PAA, 14PSS, and 14PAS). The first phosphabutadienes of any type to be generated were **4a** and **4b**, which were not isolated but thought to immediately cyclize upon formation to the corresponding 3,4-diphosphacyclobutenes.[19] In 1987, Appel and co-workers isolated three isomers of **5**.[23] The *all-trans* isomer **5c** was obtained from photolysis or thermolysis of the other two isomers. No Diels–Alder reactions of these dienes were possible, suggesting a locked *s-trans* conformation.

The optimized structures of all minimum energy isomers of **14P** are shown in Figure 1. The P=C and C—C distances in the

R—P=C(OTMS)—C(OTMS)=P—R

4a, R = *t*-Bu; **4b**, R = phenyl

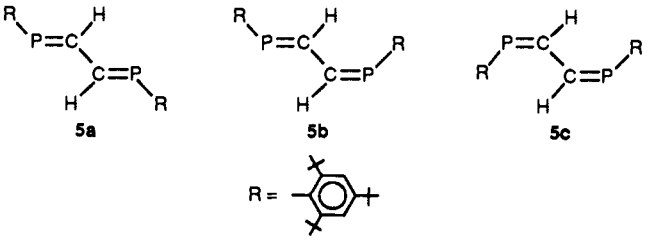

5a **5b** **5c**

R =

s-trans conformations are all identical, regardless of the stereochemistry about the P=C bonds. The same is true for all the *s-gauche* isomers. The C–C distance is longer in the *gauche* conformers than in the *trans*. At the MP2/6-31G*/HF/6-31G* level, the *trans* isomers are essentially degenerate. The gauche isomers are all about 3.1 kcal mol^{-1} above the *trans* isomers. The dihedral angles in **14PGAA**, **14PGSS**, and **14PGAS** are 39.97°, 36.51°, and 34.84°, respectively.

The rotational energy surfaces of **14PAA**, **14PSS**, and **14PAS** are all isomorphic with the surface displayed in Figure 2. The barrier heights separating the *trans* from the *gauche* rotamers for **14PAA**, **14PSS**, and **14PAS** are 8.08 (φ = 102.20°), 6.90 (φ = 97.54°), and 7.39 kcal mol^{-1} (φ = 101.9°), respectively. The *cis* structure is the transition state connecting mirror image *gauche* conformers for all three systems.

(e) 2,3-Diphospha-1,3-butadiene (23P). A substituted 2,3-diphospha-1,3-butadiene **6a** was first prepared in 1983.[20] The X-ray structure showed an *s-trans* conformation. The P=C distances are 1.692 and 1.684 Å and the P—P distance is 2.171 Å. The C–P–P angles are 100.7° and 100.3°. A second 2,3-diphospha-1,3-butadiene **6b** was not isolated but was suspected as an intermediate in the synthesis of the corresponding diphosphabicyclobutane.[24]

RR′C=P—P=CR′R

6a, R = OTMS, R′ = *t*-Bu
6b, R = TMS, R′ = phenyl

The optimized structures of **23PT** and **23PG** are shown in Figure 1. The distances are shorter than in the X-ray structure, but comparison is difficult due to the differences in substituents. Unlike **23N**, there is a *gauche* local minimum (φ = 56.46°, **23PG**) at the HF/6-31G* level. Inclusion of correlation does increase the well depth associated with this *gauche* structure. The P–P distance increases by 0.02 Å upon rotation about the P–P bond from **23PT** to **23PG**, a fairly large increase suggesting significant loss of π-delocalization.

The rotational surface of **23P** is drawn in Figure 6. The global minimum is **23PT** and **23PG**, the other local minimum lies 3.05 kcal mol^{-1} higher. The barrier separating these two occurs at φ = 79.08° and is 3.45 kcal mol^{-1}. The *cis* structure lies 3.12 kcal mol^{-1} above **23PG** and is the highest energy point on the entire rotational surface.

Discussion

The principal factors determining the shape of the rotational energy surfaces of 1,3-butadienes are π-delocalization and 1,4-steric interactions.[45] Conjugation is best when the p-orbitals are perfectly aligned (φ = 0° and 180°) and is nil when the orbitals are orthogonal (φ = 90°). Steric interactions between groups attached to the 1 and 4 positions are at a maximum in the *s-cis* conformation and decrease monotonically as φ increases to 180°. Playing these two effects off each other results in the typical curve given in Figure 2. The global minimum occurs at φ = 180°; the energy rises as the angle decreases (loss of π-delocalization) until a maximum is reached (around 90°) and then the energy decreases as delocalization increases. The counterplay of increasing steric energy and increasing conjugation as φ approaches 0° results in

(45) Kavana-Saebo, K.; Saebo, S.; Boggs, J. E. *J. Mol. Struct. (THEOCHEM)* **1984**, *106*, 259–269.

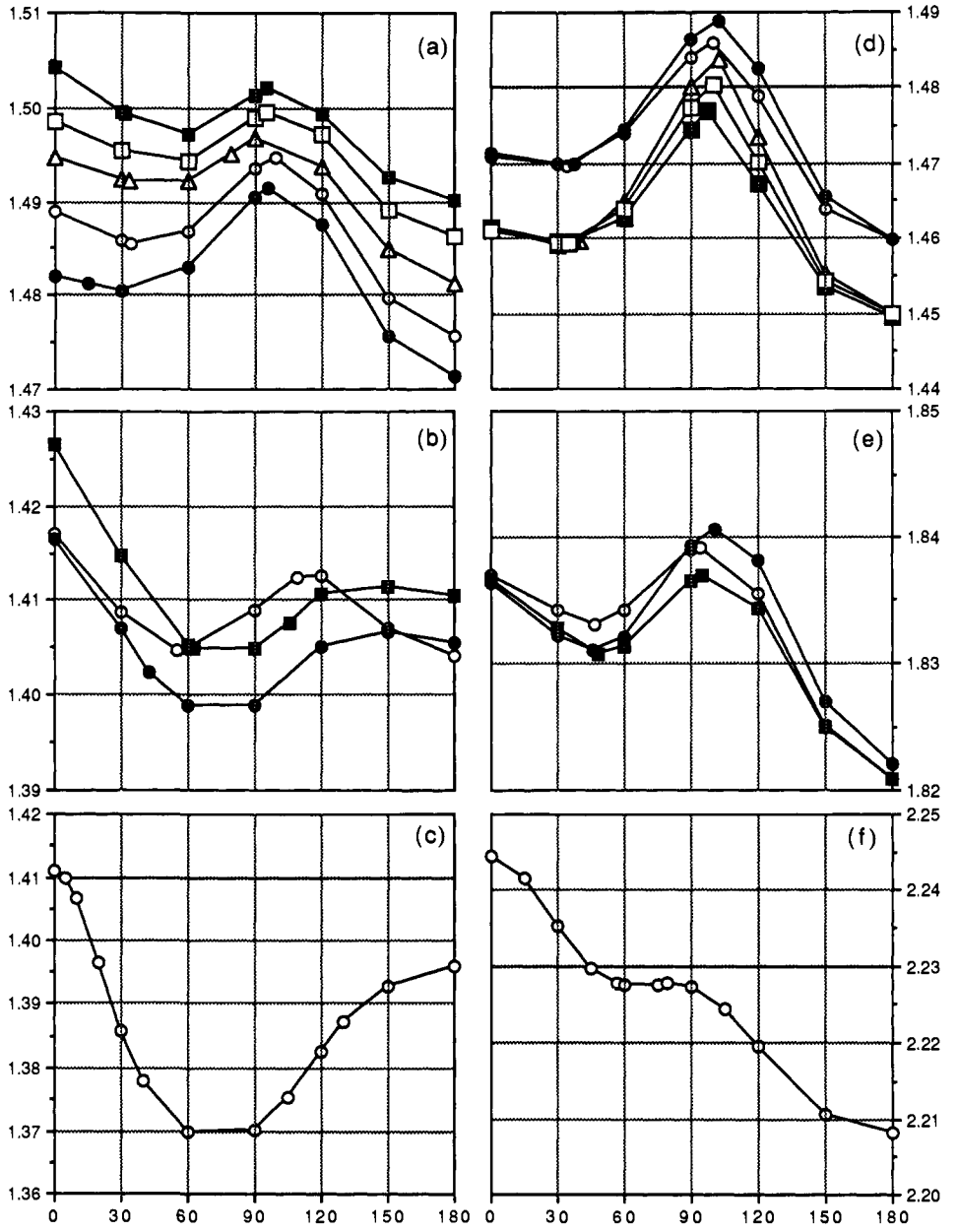

Figure 7. Plot of single bond distance vs dihedral angle: (a) C—C distance in (○) **1NS**, (●) **1NA**, (■) **14NSS**, (△) **14NAA**, (□) **14NAS**; (b) C—N distance in (○) **2N**, (●) **13NA**, (■) **13NS**; (c) N—N distance in (○) **23N**; (d) C—C distance in (○) **1PS**, (●) **1PA**, (■) **14PSS**, (△) **14PAA**, (□) **14PAS**; (b) C—P distance in (○) **2P**, (●) **13PA**, (■) **13PS**; (c) P—P distance in (○) **23P**.

a local energy minimum *gauche* structure. The planar *s-cis* conformer is a transition state separating the mirror image *gauche* conformers.

Wiberg has calculated the rotational surface of 1,3-butadiene at MP2/6-31G*//MP2/6-31G*. The *trans* to *gauche* barrier is about 5.8 kcal mol^{-1} and the *cis* structure is 3.59 kcal mol^{-1} less stable than the *trans* conformer. The rotational surfaces of **1NS** and **14NSS** differ very little from those of 1,3-butadiene. Substituting N for C at the terminal position causes little change in the degree of conjugation. The degree of conjugation can be seen in examining the variation of single-bond distance with dihedral angle. These plots are shown in Figure 7. While the short C–C distance in 1,3-butadiene has been ascribed not only to conjugation but also to the sp^3 hybridization,[1] hybridization should change quite minimally with variation in the dihedral angle (particularly in the region between 90° and 180°).[15] A qualitative feel for the energetic consequences of conjugation can therefore be obtained from these plots.

For 1,3-butadiene, the C–C distance is shortest in the *trans* form and increases as φ decreases (decreasing delocalization), becoming a maximum around $\varphi = 90$. As the angle becomes smaller, the distance decreases as conjugation becomes more favorable. However, as φ approaches 0, the C–C distance increases again, reflecting the 1,4-steric interference. The C–C distance varies between 1.456 and 1.481 Å. The curves shown in Figure 7a reflect this same behavior.

The rotational energy surface of **14NAA** is isomorphic with the standard curve; however, the relative energies of the critical points are very different from those in **1NS** and **14NSS**. The rotational barrier is 8.64 kcal mol^{-1} and the *gauche* and *cis* isomers lie very high in energy. This difference can be understood in terms of 1,4-N lone-pair repulsion. In **14NAA**, the two lone pairs are *syn* to the C–C bond and will approach each other as φ approaches 0. On the other hand, the lone pairs in **14NSS** are *anti* to the C–C bond and will remain far apart as φ changes. This can be seen by comparing the *cis* structures **7** and **8**. The relatively flat energy curve of **14NAA** between $0° < \varphi < 90°$ reflects the balance of increased conjugation as φ approaches zero against increased lone-pair repulsions.

2N and **13NS** have normal-type rotational energy surfaces, but with low rotational barriers and very energetic *cis* conformers. In fact, the *cis* conformers are the maximum energy points on

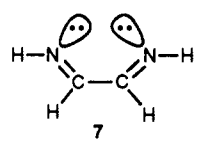

7

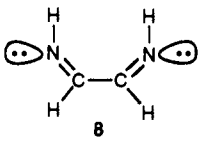

8

the surfaces. The very low rotational barrier results from electron delocalization still active even when $\varphi \approx 90°$. The C–N distance in **2N** increases less than 0.005 Å in the progression from φ = 180° to 90°, while the C–N distance in **13NS** is actually smaller at φ = 90° than in the *trans* conformer. Conjugation when the dihedral angle is near 90° does not occur between the two double bonds, which are, of course, orthogonal. Rather, conjugation occurs between one π^*-orbital and the N lone pair, as shown in 9. The *cis* conformers are destabilized by 1,4-steric interactions that are larger than in 1,3-butadiene due to the substitution of N for C in the 2 or 3 position. The bond angle about this N is smaller than that for C, bringing the 1 and 4 groups closer together.

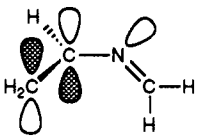

9

The other azabutadienes have rotational surfaces that deviate strongly from the normal type. Something besides conjugation and 1,4-steric interactions must act to alter the shape of the rotational surface. For **1NA** and **14NAS**, whose rotational surfaces are represented in Figure 3, hydrogen bonding stabilizes the *cis* isomer to the extent that it becomes a local minimum and no stable *gauche* structure exists. The *cis* structures of **1NA** and **14NAS** are drawn in Figure 1 and both clearly show the proper orientation of the N lone pair and the H on position 4 for hydrogen bonding to occur. The donor H in **14NAS** is bound to N, while in **1NA** it is bound to C. The former case provides for a much more charged H and a stronger hydrogen bond than in the latter. In **1NA**, the N···H distance is 2.640 Å which is longer than a typical N···H hydrogen bond;[44] however, there is certainly some interaction. The N···H distance in **14NAS** is 2.398 Å, which is only 0.2 Å longer than typical hydrogen bonds. This short distance indicates a strong stabilizing interaction, which accounts for the near degeneracy of **14NTAS** and **14NCAS**.

The rotational surface for **13NA** (shown in Figure 4) is characterized by the usual four critical points, but the *gauche* minimum and the *cis* transition state both are lower in energy than the *trans* minimum. A number of factors determine the shape of this surface. While the *trans* conformer is a local minimum, the lone pairs in the 1 and 3 position are directed toward each other, which destabilizes this conformer. Rotation of the dihedral angle away from 180° will decrease the π-delocalization but also decrease this repulsion. This leads to a low barrier. The low barrier in **2N** and **13NS** implicated delocalization between the π^* orbital and the N lone pair. This effect acts in **13NA** as well and leads to a low barrier and does stabilize the *gauche* conformer. This can be seen in the very short C–N distance in the 45° < φ < 100° range (see Figure 7b). The *gauche* conformer also benefits from a weak N···H interaction. While the *cis* isomer has the strongest N···H interaction, the π^*–N lone pair interaction is lost, the C–N distance lengthens, and the energy rises above the *gauche* conformer.

The rotational surface of **23N** differs quite dramatically from that of the others. It is dominated by the very energetic *cis* conformer, which is the barrier separating the *trans* conformers. This conformer places the adjacent N lone pairs in a *cis* planar arrangement and leads to significant repulsion. The *trans* conformer minimizes the lone pair–lone pair repulsion.

The experimental studies of 2,3-diaza-1,3-butadiene show a difference from our surface in terms of the height of the *cis* barrier.[39,40] The experimental *cis* barrier is dramatically lower than that obtained by calculation. Bock[38] has criticized the experimental conclusions since a rigid-rotor model was assumed. The variation in the N–N distance with rotation is large, as shown in Figure 7. The N–N distance in the *trans* conformer is 1.396 Å and decreases to 1.37 Å for the region 60° < φ < 90°. This short distance is due to two π^*–N lone pair orbital interactions. The N–N distance increases with smaller φ, reaching a maximum of 1.411 Å in the *cis* conformation. The C–N–N angle varies over a range of 112.3° (*trans*) to 122.3° (*cis*). Clearly, the molecule does not act as a rigid rotor.

The experimental studies suggested the presence of a second isomer, having $\varphi \approx 60°$ and lying 1.2 kcal mol^{-1} above the *trans* conformer.[39,40] The previous calculations[38] found only a plateau region but no second minimum. The HF/6-31G* surface shows no second minimum, but the MP2 surface does indicate a second minimum with φ = 100°. This minimum lies 0.7 kcal mol^{-1} above the *trans* conformer and the barrier separating them is quite small. This result now brings the calculations into accord with experiment.

All isomers of the mono- and diphospha-1,3-butadienes have rotational energy surfaces that are isomorphic with the standard curve shown in Figure 2. These surfaces can be rationalized in terms of π-delocalization and 1,4-steric interactions, as described previously.

1PS, **1PA**, **14PSS**, **14PAA**, and **14PAS** have rotational barriers in the range of 7 to 8 kcal mol^{-1}. These barriers are slightly larger than the barrier in 1,3-butadiene and the analogous azabutadienes. The C–C distances in these compounds are shorter than in their aza analogues. The C–C distance in these phosphabutadienes lengthens by about 0.03 Å upon rotation to $\varphi \approx 90°$ (see Figure 7d), while the distance in the azabutadienes lengthen only 0.02 Å. This evidence suggests slightly more conjugation exists in these phosphabutadienes than in the azabutadienes. This can be rationalized in terms of the different electronegativities of P and N. Phosphorus is less electronegative than carbon, creating a polarized $C^{\delta-}$=$P^{\delta+}$ double bond. The negatively charged C will have a large HOMO coefficient which will interact strongly with the π^* of the other double bond. On the other hand, the C=N is polarized in the opposite orientation, thereby the C has a smaller HOMO coefficient, less interaction with the other π^* orbital, and therefore less conjugation than the P systems.

1PA and **14PAS** do have *gauche* minima, unlike their aza analogues which have *cis* minima. These latter minima are due to intramolecular hydrogen bonding. Phosphorus does not participate in hydrogen bonding (being positively charged and having a relatively unaccessible lone pair) and cannot stabilize the cis conformers in this fashion. Their rotational curves are therefore of the normal variety.

2P, **13PS**, and **13PA** have barriers of 3.1–3.6 kcal mol^{-1}, which are lower than the barriers presented above. For the aza analogues, this lowering was ascribed to conjugation between the lone pair and the π^* orbital, as shown in 9. This interaction occurs in the P compounds as well, but it is not quite as effective as in the N compounds. The P lone pair is less difuse and will not overlap well with the π^* orbital. This can be seen in the slightly larger rotational barriers and the lengthening of the C–P bond during rotation (Figure 7e). Unlike the N compounds, where the C–N bond is shorter at φ = 90° than in the *trans* conformer, the C–P distance lengthens at $\varphi \approx 90°$ and shortens as the dihedral angle approaches either 0° or 180°.

An alternative argument is that conjugation across the C–P single bond is small, leading to a low barrier to rotation. The C–P bond is considerably longer than the C–C or C–N bond and would reduce the overlap of the adjacent π-bonds. If no conjugation were present, a 2-fold rotational energy surface and r(C–P) vs φ curve would be anticipated. The presence of the energy maximum around 90° corresponding with the r(C–P) maximum and the presence of a *gauche* minimum argue that π-delocalization does play some role.

The difference in the rotational surfaces of **23P** and **23N** is dramatic. The **23N** surface is dominated by the very energetic *cis* conformer due to the large lone-pair repulsion. The *cis* barrier in **23P** is much lower and is attributed to two factors. First, P

lone pairs have much greater s character than N lone pairs and will be more contracted. Second, the P-P distance is about 0.8 Å longer than the N-N distance which keeps the P lone pairs well separated. The HF/6-31G* surface for **23P** does exhibit a *gauche* minimum unlike **23N**. This too is a consequence of diminished lone-pair repulsion in **23P** as compared to **23N**.

The rotational barriers of the unsubstituted phospha-1,3-butadienes examined here are all relatively small (less than 8 kcal mol^{-1}). Stable *gauche* conformers are readily accessible and lie only 1-3 kcal mol^{-1} above the global minimum *trans* conformers. There appears to be no inherent reason the phospha-1,3-butadienes cannot adopt a *gauche* (or even sample the *cis*) conformation that is needed for electrocyclic and cycloaddition reactions to occur. The dearth of reactions of this type for the acyclic phosphabutadienes must therefore arise from another source. One distinct possibility is that the currently produced phosphabutadienes possess large substituents that may sterically prevent the butadiene backbone from attaining the necessary *cis* conformation. Another possibility is that the transition state for electrocyclic and cycloaddition reactions involving phosphabutadienes is unfavorable. The former explanation appears most likely since cyclic phosphabutadienes are known to undergo pericyclic reactions.[46] We are continuing our efforts in this area and will report our results in due course.

Acknowledgment is made to the donors of the Petroleum Research Fund, administered by the American Chemical Society, for support of this research and to the National Science Foundation for equipment Grant DIR-8907135.

Registry No. 1-Aza-1,3-butadiene, 18295-52-8; 2-aza-1,3-butadiene, 38239-27-9; 1,3-diaza-1,3-butadiene, 35172-91-9; 1,4-diaza-1,3-butadiene, 40079-19-4; 2,3-diaza-1,3-butadiene, 503-27-5; 1-phospha-1,3-butadiene, 135865-42-8; 2-phospha-1,3-butadiene, 122682-85-3; 1,3-diphospha-1,3-butadiene, 134403-78-4; 1,4-diphospha-1,3-butadiene, 134403-79-5; 2,3-diphospha-1,3-butadiene, 122668-80-8.

Supplementary Material Available: Listings of **Z** matrices (HF/6-31G*) and energies of all critical points on the rotational surfaces of all compounds examined in this paper (10 pages). Ordering information is given on any current masthead page.

(46) (a) de Lauzon, G.; Charrier, C.; Bonnard, H.; Mathey, F.; Fischer, J.; Mitschler, A. *J. Chem. Soc., Chem. Commun.* **1982**, 1272-1273. (b) de Lauzon, G.; Charrier, C.; Bonnard, H.; Mathey, F. *Tetrahedron Lett.* **1982**, *23*, 511-514.

Ligand Field Strengths and Oxidation States from Manganese L-Edge Spectroscopy

S. P. Cramer,*,†,§§ F. M. F. deGroot,§ Y. Ma,‡ C. T. Chen,‡ F. Sette,‡ C. A. Kipke,⊥ D. M. Eichhorn,⊥ M. K. Chan,⊥ W. H. Armstrong,⊥ E. Libby,‡‡ G. Christou,‡‡ S. Brooker,∥ V. McKee,∥ O. C. Mullins,†† and J. C. Fuggle§

Contribution from the Department of Applied Science, University of California, Davis, California 95616, AT&T Bell Laboratories, Murray Hill, New Jersey 07974, Department of Chemistry, Indiana University, Bloomington, Indiana 47405, Research Institute for Materials, University of Nijmegen, Toernooiveld, NL-6525 ED Nijmegen, The Netherlands, Schlumberger-Doll Research, Old Quarry Road, Ridgefield, Connecticut 06877, Department of Chemistry, University of California, Berkeley, California 94720, Department of Chemistry, Canterbury University, Christchurch, New Zealand, and Division of Applied Science, Lawrence Berkeley Laboratory, Berkeley, California 94720. *Received November 5, 1990*

Abstract: $L_{2,3}$ X-ray absorption spectra have been recorded for Mn(II), Mn(III), and Mn(IV) samples with a variety of ligands. For high-spin Mn(II) complexes, a systematic variation in spectra is observed as the ligand field is increased. A dramatically different spectrum is observed for $Mn(CN)_6^{4-}$, consistent with the presence of a low-spin complex. Progressing in oxidation state from Mn(II) to Mn(III) through Mn(IV) complexes, the primary peak position shifts first 1.5-2 eV and then 1-2 eV to higher energy, and the ratio of L_3 to L_2 intensity decreases. The spectra have been quantitatively simulated with an atomic multiplet program with an octahedral crystal field superimposed. The high resolution, strong sensitivity to chemical environment and amenability to quantitative spectral shape analysis indicate that L-edges of the first transition series metals are a potentially useful probe for bioinorganic studies.

Introduction

This paper presents new data on the chemical sensitivity of manganese $L_{2,3}$ X-ray-absorption edges and discusses the potential bioinorganic applications of soft X-ray L-edge spectroscopy. Transition-metal complex $L_{2,3}$-edge spectra involve 2p → 3d transitions and hence are sensitive to factors which change 3d orbital splittings and populations.[1] Improved synchrotron radiation beam lines allow these 3d metal L-edge spectra to be probed with high resolution,[2] and soft X-ray array detectors permit

† University of California, Davis.
‡ AT&T Bell Laboratories.
‡‡ Indiana University.
§ University of Nijmegen.
†† Schlumberger-Doll Research.
⊥ University of California, Berkeley.
∥ Canterbury University.
§§ Lawrence Berkeley Laboratory.

Table I. X-ray Derived 10Dq vs Optical Values

Mn(II) complex	optical 10Dq (eV)	ref	X-ray 10Dq (eV)
$(Et_4N)_2[MnCl_4]$	-0.41	21	-0.30
MnS	0.88	22	0.60
$MnCl_2$	0.93	13	0.75
$MnCl_2$	1.03	14	
MnF_2	0.97	23	0.75
$MnSO_4$	~1.0	24	0.75
$(HB(3,5\text{-}Me_2pz)_3)_2Mn$	~1.3	24	1.05
$K_4Mn(CN)_6$	~3.7	26	3.90

0002-7863/91/1513-7937$02.50/0